Journal of Structural Geology, Vol. 16, No. 1, pp. 97 to 107, 1994
Printed in Great Britain

0191-8141/94 $06.00 + 0.00

Strain and scaling of faults in the chalk at Flamborough Head, U.K.

D. C. P. PEACOCK and D. J. SANDERSON

Department of Geology, University of Southampton, Southampton SO9 5NH, U.K.

(*Received* 10 *November* 1992; *accepted in revised form* 26 *February* 1993)

Abstract—Analysis has been made of the orientations, displacements and spacings of 1340 extensional faults, with displacements of up to 6 m, along an almost completely exposed 6 km length of cliff. This data set has been used to study how fault populations account for strain in a region and to study relationships between different scales of fault. Strains have been estimated; the maximum and intermediate extensions are sub-horizontal, with approximately equal extension ($e \approx 0.01$) in all horizontal directions. It can be inferred that the minimum extension (maximum compression) was sub-vertical, but that the wide variety of fault orientations and cross-cutting relationships resulted from variable horizontal extensions. Some faults have oblique-slip slickenside lineations, which imply a period of later, dominantly NNW–SSE extension, which possibly developed as the exposure-scale faults linked up E–W-striking larger-scale normal faults, effectively forming a single wide fault zone.

Graphs of displacement per unit distance are used to illustrate variations in displacement. The scaling of fault displacement appears to follow a power-law relationship. The differences in orientation between the small-scale and large-scale faults precludes a simple estimation of the total strain over all scales.

INTRODUCTION

AN ALMOST completely exposed 6 km length of coast has been studied along the south of Flamborough Head, Humberside, U.K. (Fig. 1), to examine how different scales of fault account for strain in a region. An early description of the faults on the south coast of Flamborough Head was given by Lamplugh (1895). This paper aims to describe four aspects of the normal faulting:

(1) the orientations of faults and slickenside lineations in the chalk and the inferred palaeostress orientations responsible for the faults;

(2) methods for describing displacement per unit distance for fault populations;

(3) possible lithological control on fault intensity in the chalk; and

(4) possible power-law relationships for scales of fault displacement and spacing.

A model is developed for the formation of the faults at Flamborough Head which incorporates these observations.

The section examined extends from the steps at Sewerby to High Stacks (Fig. 1). The cliff shows only three significant breaks; at Dykes End, at a landslide and at South Landing. The exposure consists of Upper Cretaceous chalk in cliffs up to about 40 m high. Bedding is sub-horizontal, except where drag occurs in fault zones. Gentle dome-type folding occurs (Patsoules & Cripps 1990), this being apparent on the wave-cut platform. Sub-horizontal, bedding-parallel stylolites are common. Thin marl beds occur, through which faults are often refracted (Fig. 2a). 1340 individual faults and fault zones have been identified. Most of the faults are separated into discrete, individual planes which are often segmented, with contractional (Fig. 2a) and extensional (Fig. 2b) oversteps and bends. Some faults are grouped together to form complex zones of fracturing, which are similar to the faults described by Koestler & Ehrmann (1991, figs. 2 and 4).

The following information has been collected for each fault: dip and dip direction, orientation of slickenside lineations (when visible), displacement (measured as the dip-slip separation of beds) and distance along the cliff base. The faults are studied in cross-section, and were sampled by placing a tape along the base of the cliff and noting each fault which intersected the tape. Although some irregularities occur in the position of the tape, the data comprise three-dimensional measurements of individual fault geometries and an essentially one-dimensional sample line. Faults are distinguished from joints only if they show the definite displacement of a marker bed, drag or brecciation. Small landslides occur in places, but it is possible to match beds across these areas. It is unlikely that any fault with a displacement of more than about 50 mm has been missed, except in the breaks at Dykes End, the landslide and at South Landing (Fig. 1c). It is generally difficult to resolve faults with displacements of less than about 20 mm. Another problem is caused by fracture planes associated with recent slope failure, but these can be distinguished from tectonic faults because they show a dominantly opening displacement and because they are very irregular.

FAULT AND SLICKENSIDE LINEATION ORIENTATIONS AND INFERRED PALAEOSTRESS ORIENTATIONS

Peacock & Sanderson (1992, fig. 2) used the orientations of normal faults in the chalk at Flamborough Head as an example of faulting in an approximately isotropic rock. The average dip of the faults is 64°; normal faults with dips of 60–75° are widely reported from the Cretaceous chalk of NW Europe (e.g. Bevan

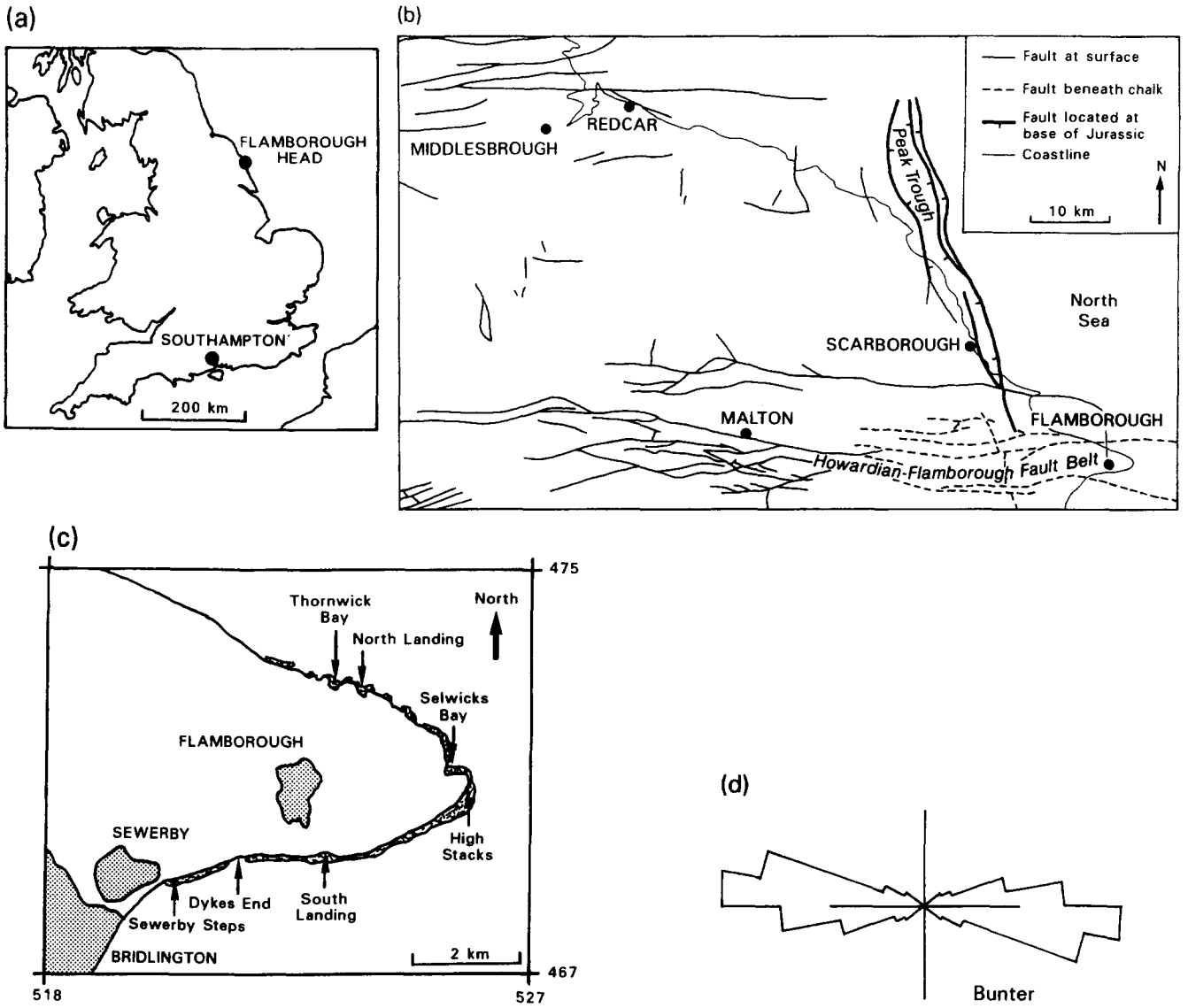

Fig. 1. (a) Map of the south of Britain, showing the location of Flamborough Head. (b) Map of the region around Flamborough Head, showing the large faults (simplified from Rawson & Wright 1992, fig. 2). Most faults strike E–W (e.g. Kirby & Swallow 1987, fig. 6), although Milsom & Rawson (1989) describe the N–S faults of the Peak Trough about 20 km to the northwest of Flamborough Head. (c) Location map for Flamborough Head. The sample line extends approximately 6 km from Sewerby (TA20166866) to High Stacks (TA25787041). The cliff shows almost complete exposure, with only three significant breaks in the sampling line; Dykes End (TA21596918, break ≈ 72 m), a landslide (TA22546917, break ≈ 90 m) and South Landing (TA23126924, break ≈ 200 m). (d) Rose diagram for fault lengths on the base of the Bunter, digitized from Amoco seismic maps for the area around Langtoft (grid reference TA010668), several kilometres to the WSW of Flamborough Head. The dominant strike of these large displacement faults is E–W.

1985, Bevan & Hancock 1986, Ameen & Cosgrove 1990, Koestler & Ehrmann 1991).

Correction of normal fault dip directions for a sampling bias

There is a wide variation in fault dip directions (Fig. 3), with individual faults on the wave-cut platform often showing sinuosity and strike variations of tens of degrees. Sampling along an ENE-trending line, imposed by the nature of the coastal exposure, has produced a bias in the data, with under-representation of faults striking at a low angle to the line (Fig. 3a). A correction can be made to the data by using the method described by LaPointe & Hudson (1985), Barton & Zoback (1990, 1992), etc. The corrected frequency (F_1) is given by:

$$F_1 = F_0/\cos\gamma,$$

where F_0 = uncorrected frequency within a range of dip directions and γ = angle between the sample line and the median value of the range of dip directions. Note that LaPointe & Hudson (1985) use the angle (Θ) between the sample line and the fracture strike. The angle (γ) between the sample line and the fault dip direction is used here to enable the distinction to be made between faults with the same strike but opposite dip directions. The correction method predicts the number of faults within a particular range of dip directions, if the sample line was reorientated to be parallel to the median value of the dip direction range. The uncorrected populations show maximum frequencies approximately parallel to the sample lines, whilst the corrected frequencies show a more even, but still irregular, distribution (Fig. 3b).

A limitation of this correction procedure is that the chance of a truly one-dimensional sample line intersecting a plane which is parallel to that line is zero. The correction for faults that dip in the direction parallel to the sample line is 1 (i.e. 1/cos 0° = 1). Where a fault strikes parallel to the sample line, the correction is infinity (i.e. 1/cos 90° = ∞). Because the data from Flamborough Head were not collected along an exactly

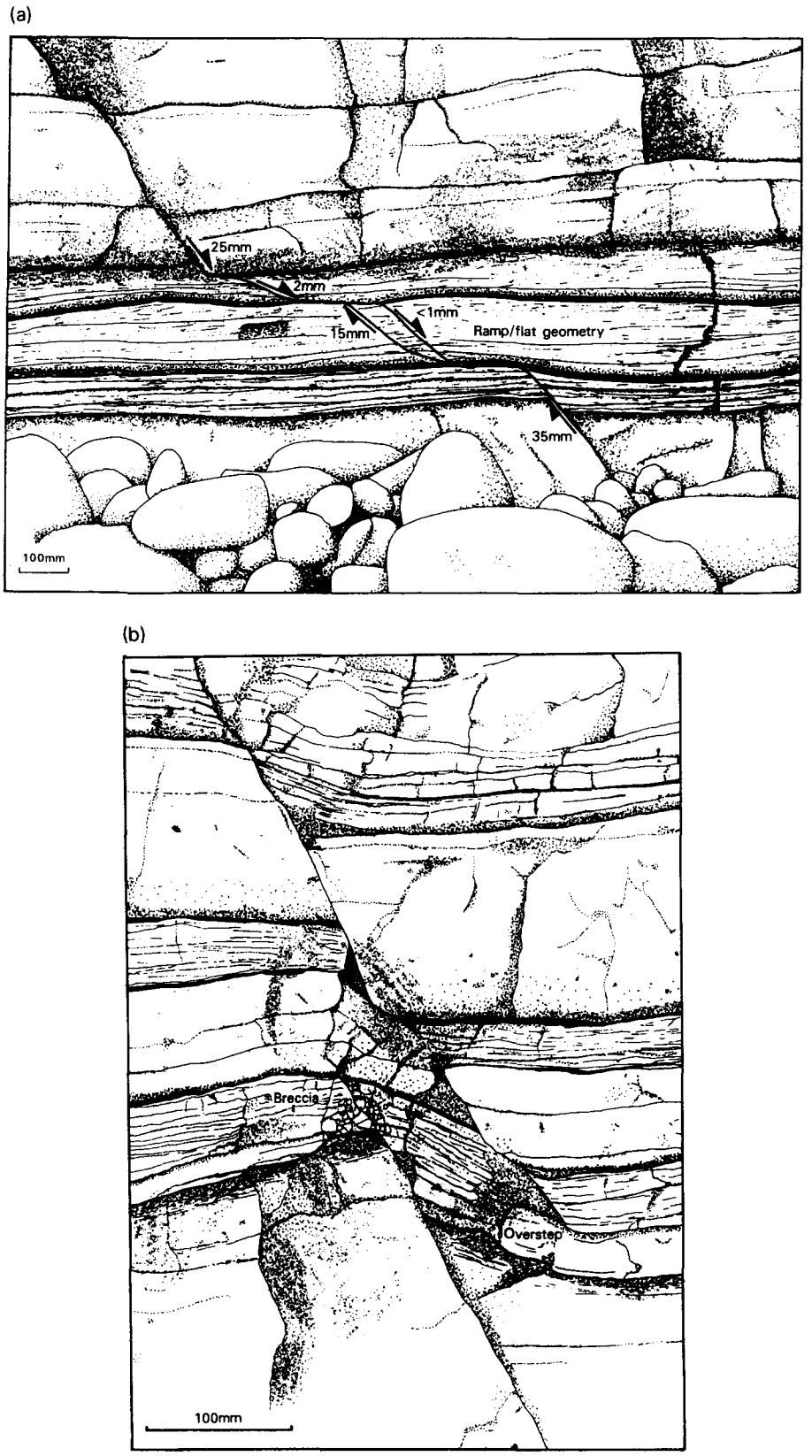

Fig. 2. (a) Example of a contractional bend. Displacement is transferred by normal drag, small-scale faults and by thinning of a marl unit. Fault displacements are measured as the dip-slip separation of beds. (b) Example of an extensional overstep. Displacement is accommodated at the overstep by a pull-apart, which is filled by folding of the beds and by some brecciation.

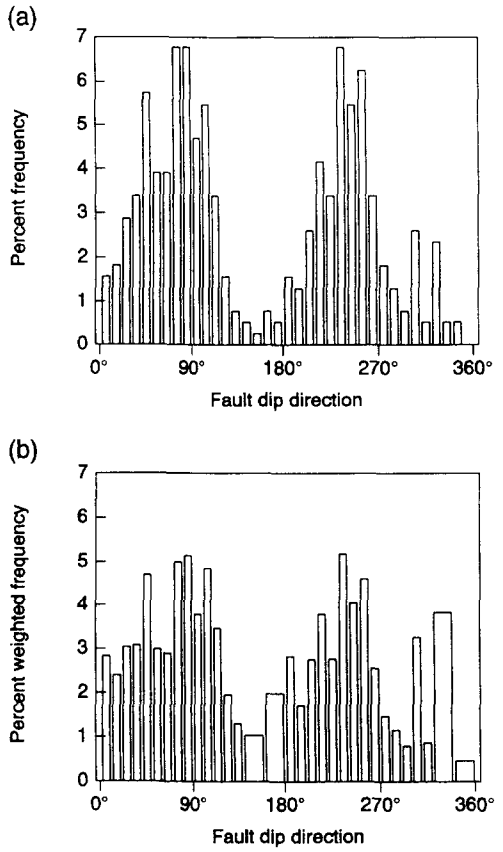

Fig. 3. Dip directions of normal faults in the chalk on the south side of Flamborough Head. (a) Bar graph of the median value of a range of fault dip directions against frequency for the 384 faults between Sewerby and Dykes End. This line sample trends at 071° and is approximately straight. (b) Corrected bar graph of the median value of a range of fault dip directions against frequency for the faults between Sewerby and Dykes End (see text for details).

straight line, faults at a low angle to the line have been over-sampled. To limit this problem, faults with a dip direction of 75–90° to the sample line are weighted by 1/cos 75°, so the weighting for each fault is never more than about 4 (Fig. 3b).

Slickenside lineation data, inferred palaeostress orientations and large-scale faults

Slickenside lineations were observed on 406 of the 1340 faults studied on the south coast of Flamborough Head; 308 of the faults have slickenside lineations with a pitch of >80°, i.e. dip-slip. These normal faults show a wide range of orientations (Fig. 4a), with the dominance of N–S-striking faults reflecting the sampling bias of an E–W-traverse. The conjugate nature of the faults and their dip-slip slickenside lineations indicate that σ_1 was sub-vertical. Figure 5 shows cross-cutting relationships for the faults along the south of Flamborough Head; the younger faults (x-axis) are those which cut relatively older faults (y-axis). Both the older and younger faults have a spread of dip directions, from 0° to 360°, with no tendency for faults in one direction to post-date those in another. The variability in the cross-cutting relationships and orientations indicates formation in a triaxial palaeostress system, with complex relationships between σ_2 and σ_3 and extension in all horizontal directions.

In addition to the dip-slip faults, 98 oblique-slip slickenside lineations (with a pitch of <80°) have been measured, with 58 having a sinistral component (Fig. 4b) and 39 having a dextral component (Fig. 4c). A few faults show both dip-slip and oblique-slip slickenside lineations. The PT dihedra method of Angelier (1984) has been used to study the oblique-slip faults; the method indicates that they formed in a palaeostress system in which σ_1 was sub-vertical, with σ_3 being sub-horizontal and orientated approximately NNW–SSE. An explanation for the slickenside lineation data at

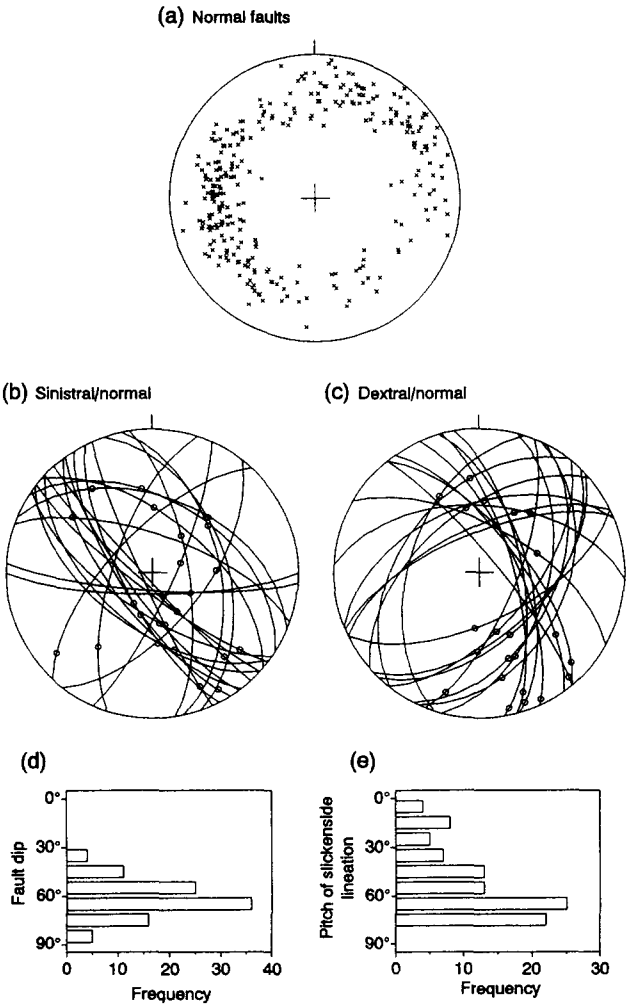

Fig. 4. Fault and slickenside lineation data for the faults between Sewerby and High Stacks (see Peacock & Sanderson 1992, fig. 2). (a) Equal-area stereogram of poles to 308 normal faults which show dip-slip slickenside lineations (pitch >80°). The faults have variable orientations, with the high frequency of N–S-trending faults being caused by measurements being taken along an E–W sampling line. East-dipping faults appear to dominate. (b) Equal-area stereogram of the 24 normal/sinistral fault planes between Sewerby and South Landing. The orientations of the slickenside lineations are also shown. Thirty four normal/sinistral fault planes were also measured between South Landing and High Stacks. (c) Equal-area stereogram of the 23 normal/dextral fault planes between Sewerby and South Landing. The orientations of the slickenside lineations are also shown. Sixteen normal/dextral fault planes were also measured between South Landing and High Stacks. (d) Histogram of fault dips for the 97 oblique-slip faults between Sewerby and High Stacks. The mean dip of 63° is similar to that for the normal faults, and may indicate that the oblique-slip faults originated as normal faults. (e) Histogram of pitches of slickenside lineations for the oblique-slip faults.

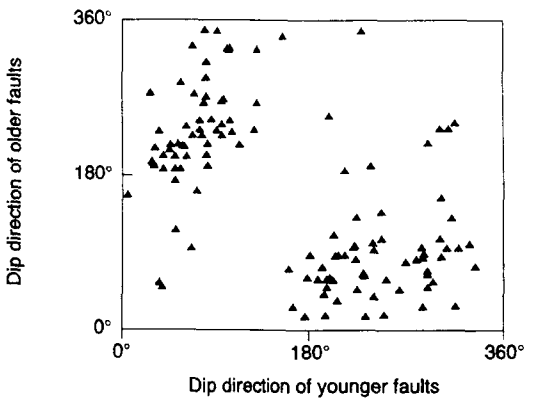

Fig. 5. Relative age relationships for pairs of cross-cutting faults at Flamborough Head shown by plotting the dip direction of older against younger faults. The scatter of data indicates a complex fault evolution and complex relationships between σ_2 and σ_3, which were sub-horizontal.

Flamborough Head is that extension in all horizontal directions produced a network of normal faults with a wide range of orientations. Later, a palaeostress system developed in which NNW–SSE extension was predominant. This produced oblique-slip on many of the pre-existing normal faults, which have various orientations. A model for the development of normal then oblique-slip faults is discussed below.

The NNW–SSE extension indicated by the oblique-slip slickenside lineations is approximately normal to the strike of the large fault zones in the region (Figs. 1b & d). An example of a large-scale fault zone occurs at Selwicks Bay, which Patsoules & Cripps (1990) believe has a normal displacement of 23 m down to the north. It is possible that different mechanisms controlled the different scale faults. Larger faults, such as the fault zone at Selwicks Bay, may have been controlled by basement structures, whereas most of the smaller faults may have been controlled by the palaeostress system with extension in all horizontal directions.

Evidence of a contractional event

The Selwicks Bay fault zone (Fig. 1c) shows evidence of both extension and contraction (Fig. 6). This ENE-striking fault zone, at the eastern end of Flamborough Head, shows a finite displacement which is normal, being about 23 m down to the north (Patsoules & Cripps 1990, Rawson & Wright 1992). Several fracture surfaces show normal or oblique displacements which indicate approximate N–S extension (Fig. 6a), reflecting this finite normal displacement. There are also many surfaces which show reverse or oblique displacements, which indicate approximate NNW–SSE contraction (Figs. 6b). The extensive calcite veining, brecciation and folding in the Selwicks Bay fault zone is probably related

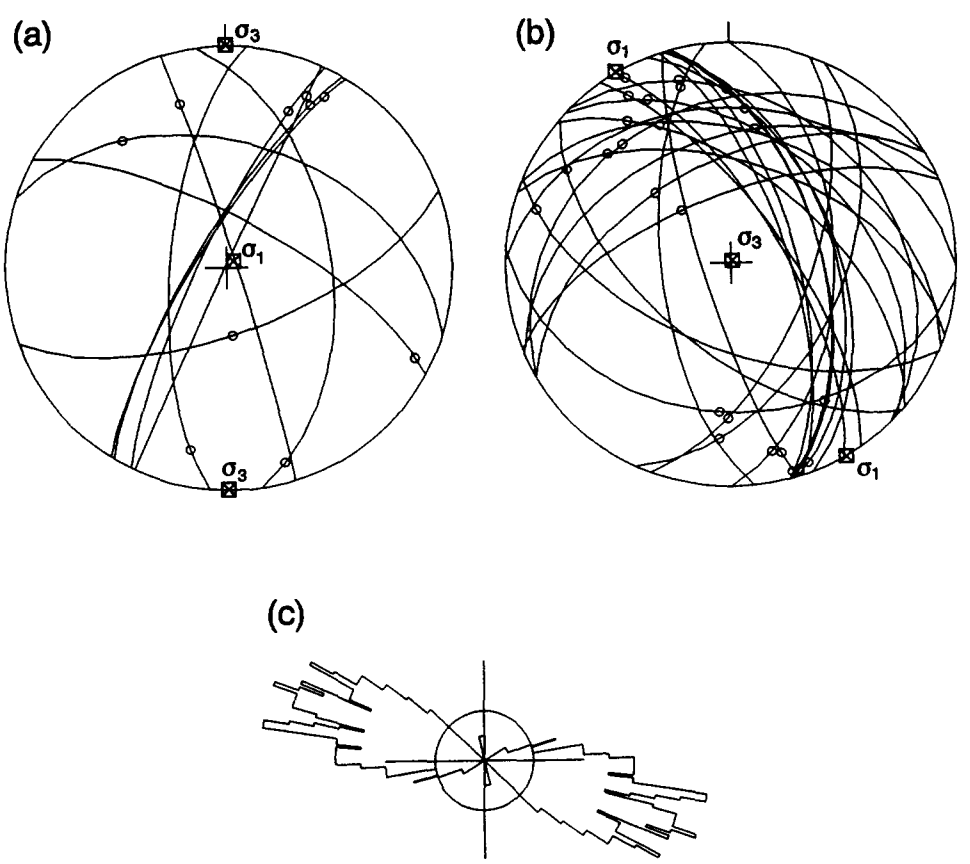

Fig. 6. Data for the Selwicks Bay fault zone (see Fig. 1c for location) and for contraction at Flamborough Head. (a) Equal-area stereogram of extensional faults and slickenside lineations at Selwicks Bay, indicating that σ_1 was sub-vertical and that σ_3 was orientated approximately NNW–SSE. (b) Equal-area stereogram of contractional faults and slickenside lineations at Selwicks Bay, indicating that σ_1 was sub-horizontal orientated approximately NNW–SSE. (c) Rose diagram of sub-vertical stylolite planes between Sewerby and South Landing. The stylolitic peaks are usually approximately perpendicular to the planes.

to the contraction. There is no visible evidence to suggest whether extension or contraction occurred first. Kirby & Swallow (1987), however, give evidence from seismic profiles through Mesozoic rocks beneath Flamborough Head of Mesozoic extension followed by end-Cretaceous or early Tertiary contraction.

A zone of contraction is also developed at Bempton cliffs on the northwest of Flamborough Head (e.g. Phillips 1829, Kirby & Swallow 1987). Small-scale folding and thrusting occurs immediately west of Danes Dyke. Rawson & Wright (1992) describe similar folding and faulting at South Landing, which is usually covered by beach deposits, and suggest that it also represents deformation above a large reactivated basement structure. These zones of contractional deformation (e.g. Selwicks Bay and Bempton cliffs) are much more localized than the normal faults, which are common around Flamborough Head. The localization of contraction could be caused by deformation above large reactivated basement structures (Rawson & Wright 1992) and/or along large pre-existing normal faults. Further evidence of contraction comes from E–W-striking sub-vertical stylolite planes with approximately perpendicular stylolitic teeth (Fig. 6c), which are common along the south coast of Flamborough Head.

DISPLACEMENT PER UNIT DISTANCE AND STRAIN

Displacement variation

Cumulative displacement–distance graphs (Chapman & Williams 1984) for the south of Flamborough Head are shown in Fig. 7. Slopes of the graphs are proportional to the displacement per unit distance which depends on the spacing and amount of displacement on the faults. For instance, a single large displacement fault at a distance of about 1.25 km from Sewerby produces a large displacement per unit distance. The form of the cumulative d–x graph also depends upon the resolution. Over large distances (Figs. 7a & b), individual faults cannot be resolved and so the profile is a moderately smooth and straight line, indicating relatively homogeneous strain at that scale of observation. The profile becomes increasingly irregular as the distance is decreased and individual faults become resolvable (Figs. 7c & d). Rutter (1986) and Wojtal (1989) show that inhomogeneous deformations (e.g. brittle structures) appear homogeneous when observed at a wider scale.

Displacement per unit distance can be plotted (Figs. 7e & f), which enables study of the variations in the rate of displacement and the homogeneity of strain. Areas of high or low displacements per unit distance are distinguishable on such graphs. The sample length determines the resolution of the graph; as the sample length increases, the resolution decreases and the graph is smoothed. Different sample lengths are shown in Figs. 7(e) & (f).

Estimating the strain ellipsoid from a single faulted line

Strain has been estimated from the fault data collected along the line sample at Flamborough Head, using a method which is fully described by Peacock & Sanderson (1993). The method is a modification of the product moment tensor method of Molnar (1983), in which displacements are weighted such that $s_1 = s_0/\cos\gamma$, where s_1 = weighted displacement on a fault, s_0 = displacement on a fault and γ = angle between the pole to the fault and the sample line. The results for the south coast of Flamborough Head are shown in Table 1. Because the amount of strain varies along the sampling line (Fig. 7), the strain estimates are averages for the three portions of the section, separated by Dykes End and South Landing. The strain estimates suggest that minimum principal extension (e_3) is sub-vertical and involves approximately 2% shortening. The maximum and intermediate principal extensions (e_1 and e_2) are consistently sub-horizontal and involve about 1% extension. This indicates approximately equal extension in all horizontal directions, as suggested by weighted estimates of fault displacements (Fig. 8) and by palaeostress orientation analysis of the normal faults (see above). The estimates for e_1 are orientated approximately NE–SW for the Sewerby to Dykes End and South Landing to High Stacks portions of the sampling line. The Dykes End to South Landing portion, however, shows an estimated e_1 orientation of approximately NNW–SSE. These variations in e_1 orientation probably occur because of the similar magnitudes of e_1 and e_2.

The strain estimates are for faults with displacements between 20 mm and 6 m. Smaller and larger displacement faults also occur, so the total strain is larger than the given estimates (Peacock & Sanderson 1993). The data collected from the south of Flamborough Head show no evidence that fault displacements (up to 6 m) vary systematically with fault orientation. Figures 1(b) and (d) show, however, that the largest faults in the region strike approximately E–W, which is compatible with the NNW–SSE extension implied by the oblique-slip faults (Fig. 4). This indicates that the different scales of faults have different orientations and magnitudes of the principal strain axes.

Possible lithological controls on faulting

Safe access to the exposure is limited on the north side of Flamborough Head, with Thronwick Bay and North Landing being the most easily accessible locations. There are fewer faults, lower displacement per unit distance and apparently fewer stylolites in the north than in the south. It is possible that the two sides of the headland are in different tectonic domains, with the north having almost no strain; the north and south coasts are separated by the Selwicks Bay fault zone. Another possible explanation for the variation is that the chalk on either side of Flamborough Head possess different mechanical properties. The chalk on the south coast is at a higher stratigraphic level (Emery *et al.* 1991, Rawson

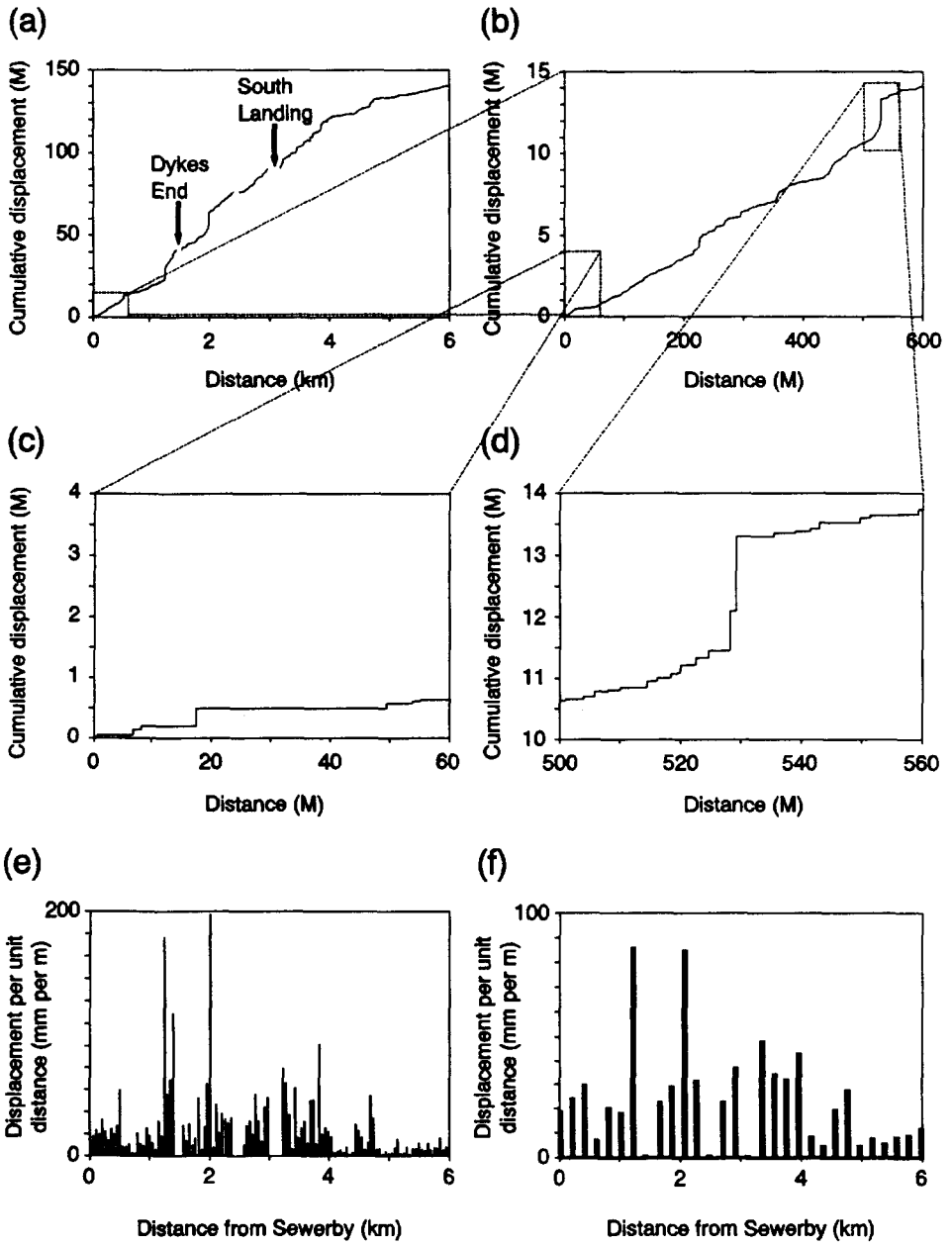

Fig. 7. Cumulative displacement–distance graphs for the 1340 normal faults between Sewerby and High Stacks. The largest fault has a displacement of about 6 m. *Cumulative displacement*, as used here, is derived by adding the dip-slip separation of beds, whatever the orientation of the faults. (a) Graph for the whole of the 6 km sample line between Sewerby and High Stacks. (b) Graph for 600 m of the sampling line. (c) Graph for 60 m of the sampling line which does not include a large (>1 m) displacement fault. (d) Graph for 60 m of the sampling line, including a relatively large (>1 m) displacement fault. Both graphs have straight portions, representing approximately homogeneous strain at that scale of observation. Between the straight portions are vertical steps which represent relatively large displacement faults and/or closely-spaced faults, i.e. strain inhomogeneity. (e) Graph of displacement per unit distance for Fig. 7(a). *Displacement per unit distance* for this graph is derived by adding the displacements on all the faults in a 50 m interval, then dividing this total by 50 m. Peaks in the graph represent areas with many faults and/or large displacement faults. (f) Graph of displacement per unit distance using a 200 m interval.

Table 1. Strain estimates for the three approximately straight sample lines along the south coast of Flamborough Head (Peacock & Sanderson 1993). The Dykes End to South Landing portion includes a 90 m break caused by a landslide

	Sewerby to Dykes End	Dykes End to South Landing	South Landing to High Stacks
Section length (m)	1449	1360	2891
Number of faults	384	396	560
e_1 Magnitude	0.01095	0.01722	0.00673
Orientation	0.8° to 259.1°	4.8° to 163.1°	1° to 0.76.5°
e_2 Magnitude	0.0086	0.01229	0.00623
Orientation	5.6° to 169°	3.1° to 253.4°	8.1° to 166.6°
e_3 Magnitude	0.01955	0.0295	0.01295
Orientation	84.3° to 357°	84.3° to 0.016.4°	81.8° to 339.4°

& Wright 1992), and appears to show less flint and more marl layers than the chalk on the north coast. Corbett *et al.* (1987) describe the mechanical stratigraphy of the Austin Chalk, Texas, and show that the fracture intensity increases as the smectite content increases. Watts (1983) describes similar variations in fracture frequencies in different levels of the chalk of the Albuskjell field of the North Sea. The ≈1% horizontal extension caused by faulting in the chalk on the south coast could be accommodated by 'ductile' (i.e. microscopic) deformation in the chalk on the north coast.

SCALING RELATIONSHIPS FOR FAULT DISPLACEMENTS AND SPACINGS

There has been much interest in the self-similarity of faulting (Tchalenko 1970, King 1983) and in the power-law relationships for different sizes of earthquakes (Scholz 1982, Turcotte 1990), fault displacements (Barton & Zoback 1990, 1992, Davy *et al.* 1990, Scholz & Cowie 1990, Marrett & Allmendinger 1991, Walsh &

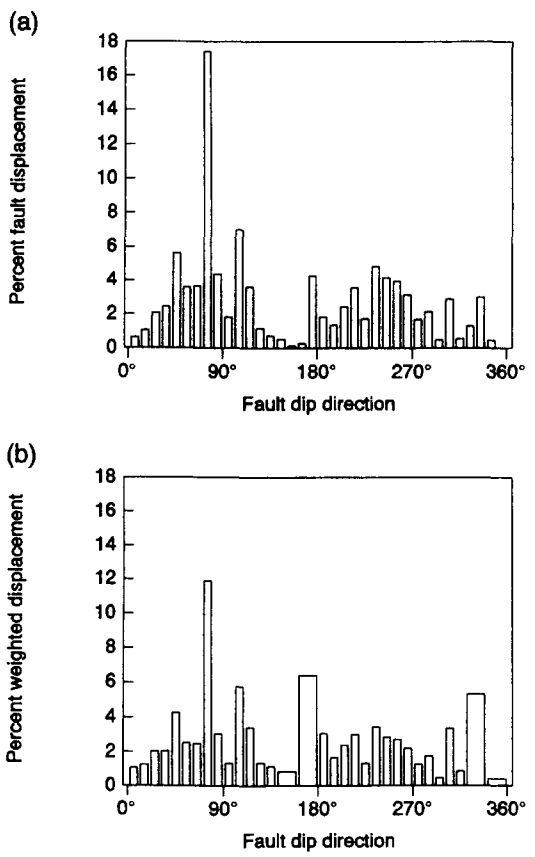

Fig. 8. Displacement data for the 384 faults between Sewerby and Dykes End, which is an approximately straight portion of the cliff, trending at 071°. The simplifying assumption is made that all of the faults have dip-slip displacements. (a) Bar graph of the median value of a range of fault dip directions against the sum of displacements in each range of fault dip directions. (b) Bar graph of the median value of a range of fault dip directions against the weighted frequencies of displacements in each range of fault dip directions. The distribution is smoothed, but is still irregular. Note that the relatively high displacements in the range 070–080° is caused by a 5 m displacement fault dipping towards 071°.

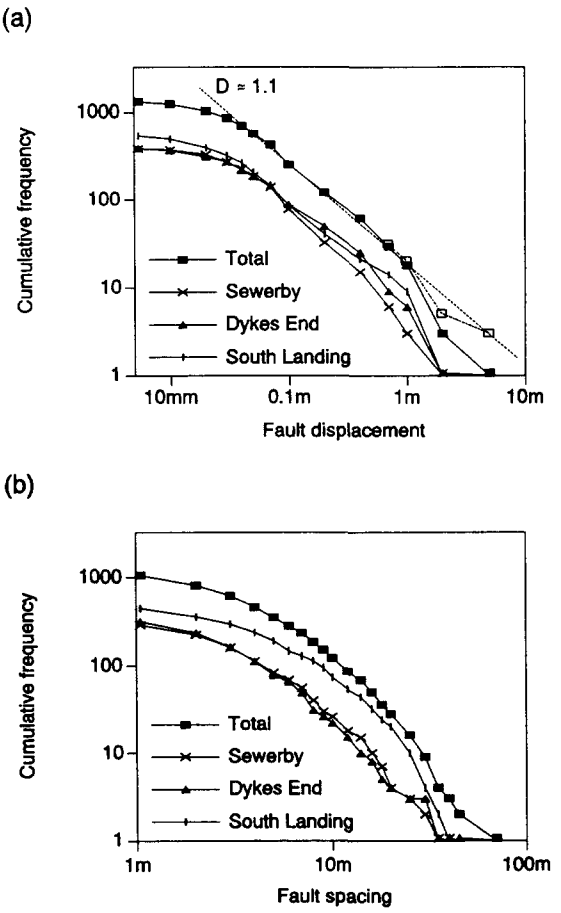

Fig. 9. Logarithmic (base 10) plots of cumulative frequency against (a) fault displacement and (b) spacing for the faults along the south coast of Flamborough Head. Graphs are shown for the total sampling line (1340 faults) and for the three portions (between Sewerby, Dykes End, South Landing and High Stacks). The displacement graphs (a) are approximate straight lines for faults with more than about 20 mm displacement, and hence show a power-law relationship. The power-law relationship is particularly apparent when the censoring effect is removed by adding two faults of more than 6 m displacement to the data (represented by the open squares). It is possible that such large displacement faults occur in the breaks of section at Dykes End and South Landing. The fault spacing graphs (b) are not straight lines, hence fault spacing does not appear to have a power-law relationship.

Watterson 1992) and fracture distributions (Hirata *et al.* 1987). The almost completely exposed 6 km length of cliff at Flamborough Head allows sampling of hundreds of faults with displacements ranging over several orders of magnitude.

The 1340 normal faults measured appear to have a power-law relationship for displacement (Fig. 9a). Measured displacements range from 5 mm to 6 m, but faults with displacements of less than about 50 mm have been under-sampled. Reliable measurements, therefore, extend over about two orders of magnitude. Barton & Zoback (1990, 1992) describe two classes of size sampling bias for displacement data. The first bias is caused by difficulty in measuring large displacements (*censoring*). It is possible that large displacement faults occur in the breaks in the sampling line (e.g. Dykes End and South Landing), but censoring does not appear to be a major problem in the Flamborough Head data. The second bias is caused by difficulty in identifying small displacement structures (*truncation*). The under-

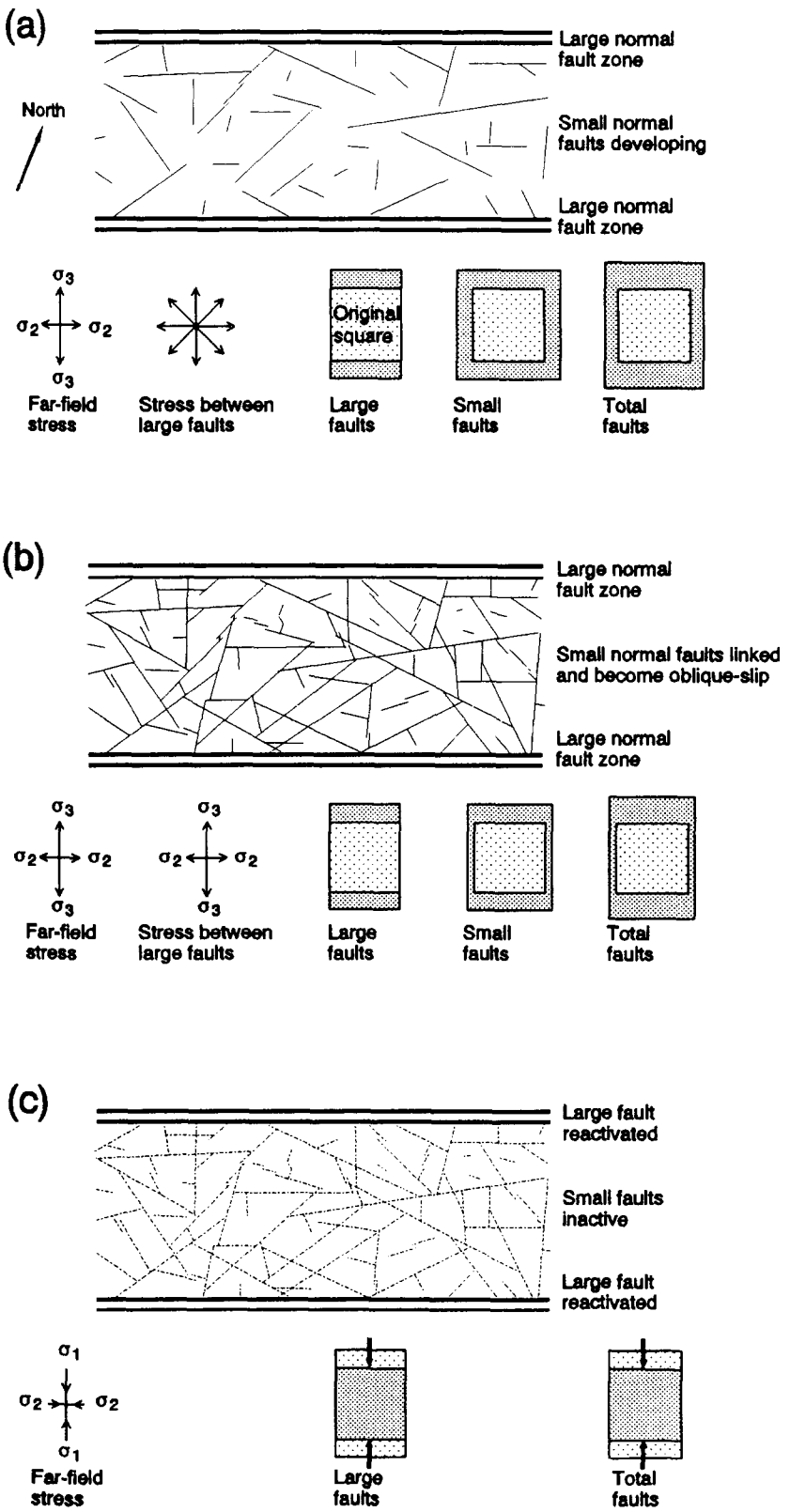

Fig. 10. Model for the development of the faults at Flamborough Head. Three stages are shown in map view. (a) The large-scale faults, probably basement-controlled, formed under a far-field palaeostress system with σ_3, and the resultant e_1, orientated approximately N–S. The deformation of an original square is shown, but note that the resultant rectangle is exaggerated. Small-scale faults develop in the areas between the large faults, where there is a complex history of palaeostress orientations in which σ_3 and σ_2 frequently change. The strain for the small faults has approximately equal extension in all horizontal directions. (b) The small-scale faults link, effectively forming a single large fault zone. Oblique-slip occurs to accommodate the approximately N–S extension. (c) The contractional (inversion) event appears to have been concentrated along basement structures and/or large normal faults, with the exposure-scale normal faults being inactive.

sampling of faults with small displacements is caused by the difficulty of observing displacements of less than about 50 mm; it is probable that many 'joints' have displacements which are too small to be measured. Patsoules & Cripps (1990) describe microfractures at Flamborough Head with displacements of up to a few microns, suggesting that the faulting extends down to sub-millimeter scale displacements.

Fault spacing does not appear to show a power-law relationship (Fig. 9b). There is no censoring effect because the maximum fault spacing is several orders of magnitude lower than the length of the sample line. Some truncation may be caused by very closely spaced faults being measured as one fault. The spacing data appears to conform better to a negative exponential distribution than to a power law.

DISCUSSION AND CONCLUSIONS

The observations on the strains and scaling of faults at Flamborough Head made in this paper may be used to develop a model for fault development, illustrated in Fig. 10. The exposure-scale normal faults have an average dip of 64°, with the data suggesting a palaeostress system in which σ_1 was sub-vertical. The wide range of fault dip directions and complex cross-cutting relationships indicates a complex relationship between σ_2 and σ_3. Strain estimated for these exposure-scale normal faults shows nearly equal extension (about 1%) in all horizontal directions. The variable orientations of the exposure-scale faults do not reflect the dominant E–W trend of the large displacement faults, which imply maximum extension orientated N–S. The differences between the strains for the exposure-scale and larger-scale faults can be explained using a model similar to that of Simon *et al.* (1988), who presented analogue and mathematical models, together with field examples, of the swapping of the σ_2 and σ_3 axes adjacent to pre-existing faults in a multidirectional extension field. At Flamborough Head, the far-field σ_3 is interpreted to have been approximately N–S, but stress release on the large normal faults caused approximately equal horizontal palaeostresses in the areas in between. This resulted in the complex pattern of small-scale faults, with approximately equal extension in all horizontal directions (Fig. 10a).

Some of the exposure-scale normal faults show oblique-slip displacements, with the slickenside lineations indicating NNW–SSE extension, i.e. the faults extend bedding but the slickenside lineations have a pitch of <80°. Some faults show both dip-slip and oblique-slip slickenside lineations, but the chronology is difficult to determine. These oblique-slip faults indicate a NNW–SSE orientation of σ_3 (Fig. 4), which may have developed in the areas where the smaller normal faults linked up to effectively form a single wide fault zone (Fig. 10b).

There is evidence of a contractional event in which σ_1 was orientated approximately N–S. The deformation produced by this event is much more localized that the extension, probably being largely confined to the regions adjacent to some of the large normal faults (Fig. 10c). This reverse reactivation appears to be selectively controlled by the larger faults.

Graphs of displacement per unit distance illustrate the concentrations of faults and the variability of displacement in an area. The outcrop-scale faults represent approximately homogeneous strain over long sampling lines. As the length of the sample line is decreased, the strain becomes more heterogeneous.

There are a large number of faults in the chalk along the south side of Flamborough Head, with far fewer occurring along the north side, which is stratigraphically lower. This may be because the two areas are in tectonically different regimes, or may be the result of mechanical variations in the chalk sequence.

Fault displacements appear to have a power-law relationship, whilst fault spacing does not. Marrett & Allmendinger (1991) show how power-law relationships for fault displacement can be used to estimate the total strain in a region, taking all scales of fault displacement into account. This suggests that it may be possible to modify the estimated strain ellipsoid to include the faults with displacements outside the range of displacements used to derive the ellipsoid. There is, however, a problem with this approach. At Flamborough Head, the faults with displacements in the range 5 mm to 6 m imply approximately equal extension in all horizontal directions (e.g. Fig. 8 and Table 1), whereas the larger displacement faults strike approximately E–W (Figs. 1b & d). The different scales of fault may therefore have strain ellipsoids with different orientations and relative magnitudes of the principal strains. The fault patterns and resultant strains do not appear to be scale-invariant. The only valid approach would be to derive, then add, strain ellipsoids for the different scales of faults.

The model presented in Fig. 10 suggests that there are complex relationships between the patterns and scaling of small-scale fractures and larger-scale fractures. This has important implications when, for example, using seismic data to evaluate the fracture patterns in hydrocarbon reservoirs.

Acknowledgements—Work for this paper was funded by Amoco through the Earth Resources Institute. Tom Patton and Randy Marrett are thanked for their help, and the comments by Antonio Casas-Sainz and an anonymous reviewer are greatly appreciated.

REFERENCES

Ameen, M. S. & Cosgrove, J. W. 1990. Kinematic analysis of the Ballard fault, Swanage, Dorset. *Proc. Geol. Ass.* **101**, 119–129.

Angelier, J. 1984. Tectonic analysis of fault slip data sets. *J. geophys. Res.* **89**, 5835–5948.

Barton, C. A. & Zoback, M. D. 1990. Self-similar distribution of macroscopic fractures at depth in crystalline rock in the Cajon Pass scientific drillhole. In: *Rock Joints* (edited by Barton, C. A. & Stephansson, O.). Balkema, Rotterdam, 163–170.

Barton, C. A. & Zoback, M. D. 1992. Self-similar distribution and properties of macroscopic fractures at depth in crystalline rock in the Cajon Pass scientific drill hole. *J. geophys. Res.* **97**, 5181–5200.

Bevan, T. G. 1985. A reinterpretation of fault systems in the Upper Cretaceous rocks of the Dorset coast, England. *Proc. Geol. Ass.* **96**, 337–342.

Bevan, T. G. & Hancock, P. L. 1986. A late Cenozoic regional mesofracture system in southern England and northern France. *J. geol. Soc. Lond.* **143**, 355–362.

Chapman, T. J. & Williams, G. D. 1984. Displacement–distance methods in the analysis of fold–thrust structures and linked fault systems. *J. geol. Soc. Lond.* **141**, 121–128.

Corbett, K., Friedman, M. & Spang, J. 1987. Fracture development and mechanical stratigraphy of Austin Chalk, Texas. *Bull. Am. Ass. Petrol. Geol.* **71**, 17–28.

Davy, Ph., Sornette, A. & Sornette, D. 1990. Some consequences of a proposed fractal nature of continental faulting. *Nature* **348**, 56–58.

Emery, L. H., Horne, M. J. & Whitham, F. 1991. *The Upper Cretaceous Chalk Formations of Humberside and North Yorkshire. Flamborough Coast Area*. Guide to Yorkshire Geological Society field meeting.

Hirata, T., Satoh, T. & Ito, K. 1987. Fractal structure of spatial distribution of microfracturing in rock. *Geophys. J. R. astr. Soc.* **90**, 369–374.

King, G. C. P. 1983. The accommodation of large strains in the upper lithosphere of the Earth and other solids by self-similar fault systems: the geometric origin of *b*-value. *Pure & Appl. Geophys.* **121**, 761–815.

Kirby, G. A. & Swallow, P. W. 1987. Tectonism and sedimentation in the Flamborough Head region of north-east England. *Proc. Yorks. geol. Soc.* **46**, 301–309.

Koestler, A. G. & Ehrmann, W. U. 1991. Description of brittle extensional features in chalk on the crest of a salt ridge (NW Germany). In: *The Geometry of Normal Faults* (edited by Roberts, A. M., Yielding, G. & Freeman, B.). *Spec. Publs geol. Soc. Lond.* **56**, 113–123.

Lamplugh, G. W. 1895. Notes on the white chalk of Yorkshire. *Proc. Yorks. geol. Soc.* **13**, 65–87.

LaPointe, P. R. & Hudson, J. A. 1985. *Characterization and Interpretation of Rock Mass Joint Patterns. Spec. Publ. geol. Soc. Am.* **199**.

Marrett, R. & Allmendinger, R. W. 1991. Estimates of strain due to brittle faulting: sampling of fault populations. *J. Struct. Geol.* **13**, 735–738.

Milsom, J. & Rawson, P. F. 1989. The Peak Trough—a major control on the geology of the North Yorkshire coast. *Geol. Mag.* **126**, 699–705.

Molnar, P. 1983. Average regional strain due to slip on numerous faults of different orientations. *J. geophys. Res.* **88**, 6430–6432.

Patsoules, M. G. & Cripps, J. C. 1990. Survey of macro and microfracturing in Yorkshire chalk. In: *Chalk* (edited by Burland, J. B., Mortimore, R. N., Roberts, L. D., Jones, D. L. & Corbett, B. O.). Thomas Telford, London, 89–93.

Peacock, D. C. P. & Sanderson, D. J. 1992. Effects of layering and anisotropy on fault geometry. *J. geol. Soc. Lond.* **149**, 793–802.

Peacock, D. C. P. & Sanderson, D. J. 1993. Estimating strain from fault slip using a line sample. *J. Struct. Geol.* **15**, 1513–1516.

Phillips, J. 1829. *Illustrations of the Geology of Yorkshire; Part* 1—*The Yorkshire Coast*. London.

Rawson, P. F. & Wright, J. K. 1992. *The Yorkshire Coast*. Geol. Assoc Guide No 34.

Rutter, E. H. 1986. On the nomenclature of mode of failure transitions in rock. *Tectonophysics* **122**, 381–387.

Scholz, C. H. 1982. Scaling laws for large earthquakes: consequences for physical models. *Bull. seism. Soc. Am.* **72**, 1–14.

Scholz, C. H. & Cowie, P. A. 1990. Determination of total strain from faulting using slip measurements. *Nature* **346**, 837–839.

Simon, J. L., Seron, F. J. & Casas, A. M. 1988. Stress deflection and fracture development in a multidirectional extension regime. Mathematical and experimental approach with field examples. *Annals Tectonicae* **2**, 21–32.

Tchalenko, J. S. 1970. Similarities between shear zones of different magnitudes. *Bull geol. Soc. Am.* **81**, 1625–1640.

Turcotte, D. L. 1990. Implications of chaos, scale-invariance, and fractal statistics in geology. *Palaeogeog., Palaeoclim., Palaeoecol.* **89**, 301–308.

Walsh, J. J. & Watterson, J. 1992. Populations of faults and fault displacements and their effects on estimates of fault-related regional extension. *J. Struct. Geol.* **14**, 701–712.

Watts, N. L. 1983. Microfractures in chalks of Albuskjell field, Norwegian sector, North Sea: possible origins and distribution. *Bull. Am. Ass. Petrol. Geol.* **67**, 201–234.

Wojtal, S. 1989. Measuring displacement gradients and strains in faulted rocks. *J. Struct. Geol.* **11**, 669–678.